Sub-10 fs spectroscopy of K-TCNQ crystal for observation of intramolecular vibration modulation in melting of the Peierls dimer

Kazuaki Nakata,[1] Eiji Tokunaga,[1] Juan Du,[2,3] Bing Xue,[2,3] Jun Miyazaki,[2,3] Keisuke Seto,[2,3] and Takayoshi Kobayashi[2,3,4,5]

[1]*Department of Physics, Faculty of Science, Tokyo University of Science, 1-3 Kagurazaka, Shinjuku, Tokyo 162-8601, Japan*

[2]*Advanced Ultrafast Laser Research Center and Department of Engineering Science, The University of Electro-Communications, 1-5-1 Chofugaoka, Chofu, Tokyo 182-8585, Japan*

[3]*Core Research for Evolutional Science and Technology (CREST), Japan Science and Technology Agency, K's Gobancho, 7, Gobancho, Chiyoda-ku, Tokyo 102-0076, Japan*

[4]*Department of Electrophysics, National Chiao-Tung University, Hsinchu 300, Taiwan*

[5]*Institute of Laser Engineering, Osaka University, 2-6 Yamada-oka, Suita, Osaka 565-0971, Japan*

(Received 30 January 2014; revised manuscript received 22 July 2014; published 14 August 2014)

K-TCNQ crystals show photoinduced phase transition (PIPT) between a Mott insulator and a spin Peierls (SP) phase, having $T_c = 395$ K (= and the crystal has $T_c = 395$ K of the PIPT). We report the intra-molecular vibrations in the excited K-TCNQ crystal after impulsive excitation using a sub 9.4 fs pulse laser in the reflection spectrum. The frequencies of the vibrations are close to the Raman frequencies of molecules. The frequencies increase with melting of the SP phase, and then decrease with rearrangement of the dimerization. In addition, the frequencies of the vibrations are time-resolved to be modulated by the intermolecular optical phonon with 510 fs period corresponding to 65 cm^{-1}. This modulation is associated with the periodical change of coupling strengths of intermolecular charge transfer and/or the dipolar coupling between the counterpart molecules in the neighboring chains.

DOI: 10.1103/PhysRevB.90.085119 PACS number(s): 78.40.Me, 78.47.−p, 82.50.−m

I. INTRODUCTION

Photoinduced phase transition (PIPT) in various materials have been attracting the interest of many scientists in the field of solid-state physics, materials science, and synthetic chemistry [1–3], and PIPT materials are expected to be useful in future optical devices.

It is well known that the phase transition is observed in the aligned alkali-organic molecules. It was claimed that the alkali-TCNQ crystals are considered to be of the generalized Peierls type crystal, because those compounds have high value of T_c and exchange interaction [4]. These characters suggest that the transition of K-TCNQ is considered to be the generalized Peierls type. In the K-TCNQ crystals, adjacent to TCNQ molecules, each of which has magnetic spin $S = 1/2$ because the charge is transferred to the TCNQ from the potassium, make a spin dimer at low temperature such that the magnetization disappears. This salt crystal has a one-dimensional face-to-face stacking structure, and the photoinduced generalized Peierls melting occurs under laser excitation as in other alkali-metal-TCNQ crystals. The transition temperature T_c between the insulator state and the generalized Peierls state in the K-TCNQ crystal is 395 K, hence the phase transition physics with laser irradiation can be investigated at room temperature. In addition, they are the organic charge-transfer compounds [4–11]. Ikegami *et al.* reported the pump-probe spectroscopy of K- and Na-TCNQ crystals in the IR region with 130 fs laser pulses generated by OPA [12,13]. They claimed that electron-hole pairs generated by photoexcitation melt the generalized Peierls phase to induce intermolecular coherent oscillations. However, the experimental time resolution was only 180 fs at best because of the 130 fs duration of the pulse from a conventional optical parametric amplifier (OPA) They found one short-lived ($\tau = 5.7$ ps) oscillation with frequency of 20 cm^{-1}, and two characteristic fast-decaying ($\tau \leqslant 600$ fs) oscillations with frequencies of 49 and 90 cm^{-1}. The oscillation with the frequency of 20 cm^{-1} coincides with the LO phonon oscillation observed in Raman spectroscopy, while the other two oscillations are assigned to the local phonon modes in the photoexcited states. However, the temporal resolution is not enough to reveal the intramolecular vibration [12–17]. In this study we could resolve the intramolecular vibration in the excited K-TCNQ crystal in real time after impulsive excitation using 9.4 fs pulses. Three prominent vibrational mode frequencies obtained by the FFT of real-time vibration amplitudes are compared with the previous Raman experiments. Finally, the delay time dependence of the instantaneous vibrational frequencies of sevearl prominent modes shows that the frequencies are modulated by the crystal TO phonon via a mode coupling.

II. MATERIAL AND METHOD

In this experiment both pump and probe pulses are generated from a noncollinear optical parametric amplifier (NOPA) laser system that is seeded by a white-light continuum [18–20]. The pulse duration of the NOPA output is 9.4 fs and covered the spectral range extending from 550 to 720 nm. The pump and probe laser powers are 30 and 5 μW, respectively.

The pump-probe reflection spectra are detected by the combined system of a polychromator with a multichannel lock-in amplifier. The spectral resolution of the total system is ∼1.5 nm. The wavelength dependent difference absorbance of the probe at 128 wavelengths is measured by changing the pump-probe delay times from −200 to 1800 fs with a 0.2-fs step. All the experiments are performed at a constant temperature (293 K).

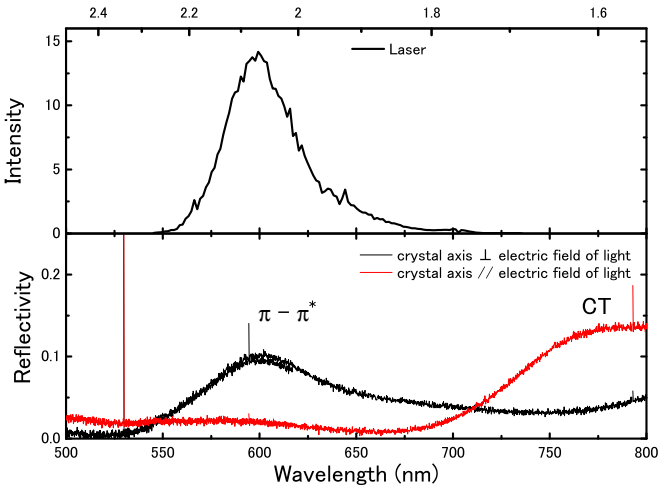

FIG. 1. (Color online) 9.4 fs NOPA laser spectrum and reflection spectrum of the K-TCNQ crystal.

A K-TCNQ crystal used in this study is made by recrystallization at 50 °C from the liquid phase reaction after mixing KI and TCNQ acetonitrile solutions. The sample is a needlelike crystal and the size is 5 mm × 0.5 mm × 0.5 mm. The reflection spectra of the crystal and the pump and probe spectra are shown in Fig. 1. The polarization in the pump and probe light are perpendicular to the stacking (a) axis in the K-TCNQ crystal.

III. RESULTS

Figure 2 shows the two-dimensional (energy − delay time) difference reflection spectrum in K-TCNQ crystal. We can find the oscillatory behavior of difference absorbance in Fig. 2. The oscillation is induced by the impulsive excitation with the pump pulse that triggers both intermolecular lattice vibration and the intramolecular oscillation in TCNQ molecules in the crystal.

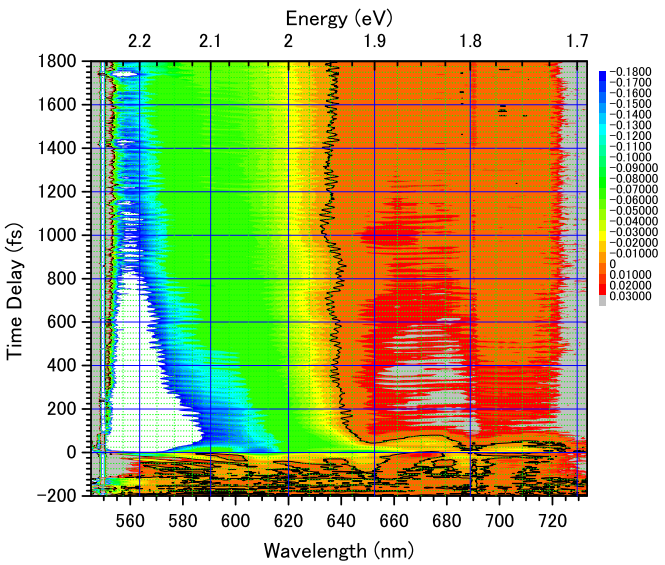

FIG. 2. (Color online) Two-dimensional $\Delta R/R$ spectrum in K-TCNQ crystal.

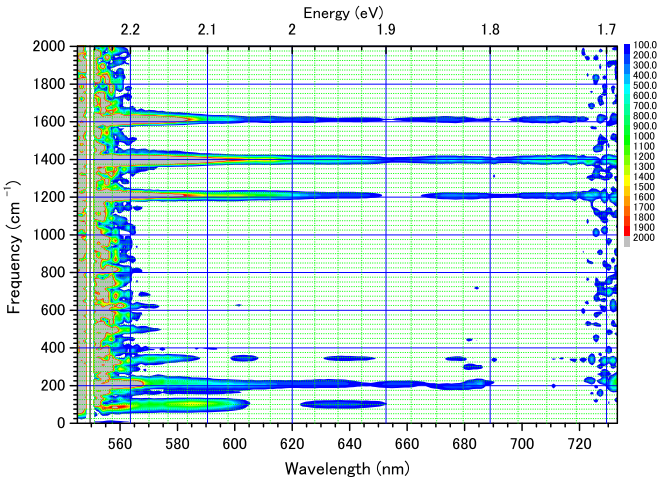

FIG. 3. (Color online) Two dimensional (energy−frequency) FFT power spectrum calculated from time dependence absorbance change.

Figure 3 shows the two-dimensional (probe photon energy−vibration frequency) FFT power spectrum obtained by the same measurement as in Fig. 2. Several characteristic frequencies in the excited K-TCNQ crystal are shown in Fig. 3. In this paper we report the observation of real-time intramolecular vibrational modes in the TCNQ molecules.

Time-resolved reflection spectra are shown in Fig. 4. Reflectivity changes below 1.92 eV increase with delay time, while those above 1.94 eV decrease.

Figure 5 shows the time traces in the energy region of interest. To determine the decay times, these time profiles were fitted with two exponential decay functions. The shortest exponential decay component in these two have the time constant of 80 ± 33 fs and that of the second component is 570 ± 19 fs.

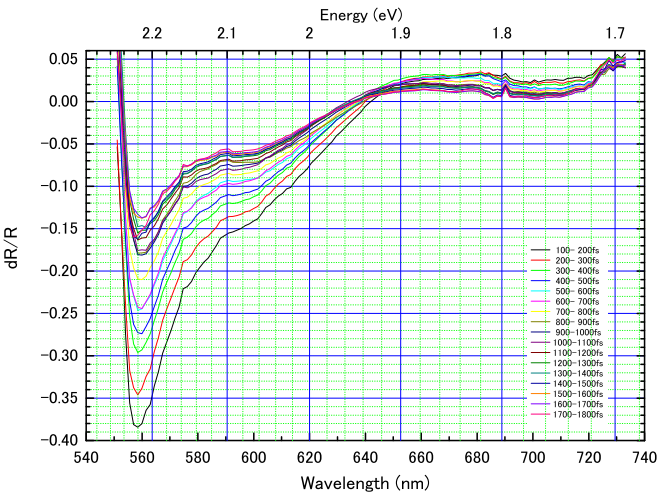

FIG. 4. (Color online) Time-resolved reflection spectrum of the K-TCNQ crystal.

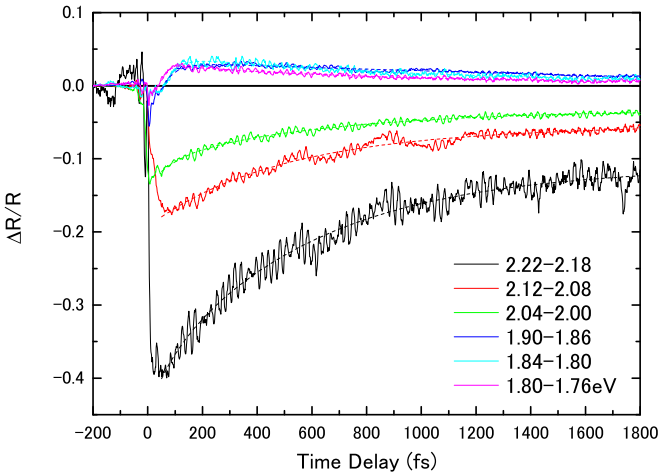

FIG. 5. (Color online) Time traces $\Delta R/R$ in several energy ranges.

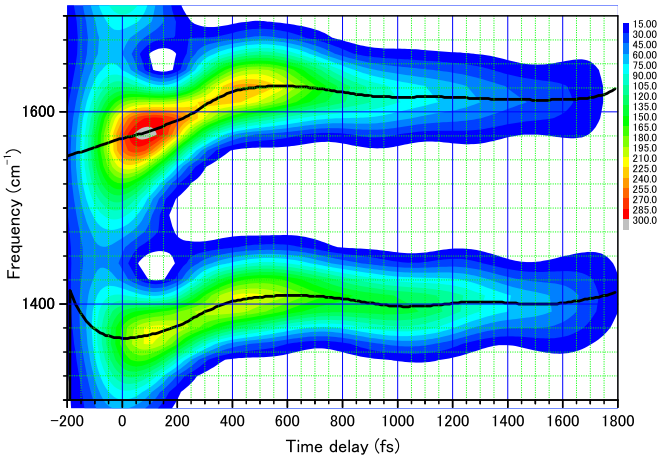

FIG. 6. (Color online) Spectrogram analysis in 2.22–2.18 eV energy region in $\Delta R/R$ spectrum with a Blackman window, width 900 nm.

IV. DISCUSSION

In Fig. 5 a short decay time, $\tau_1 = 80$ fs, and a long one, $\tau_2 = 570$ fs, are determined. The determination of short time constant suffers from error due to the coherent spike. The second component ($\tau_2 \sim 500$ fs) represents the time for the generalized Peierls phase to melt with the excitation laser. This decay time is close to that reported previously by the pump-probe experiment with IR, or CT, excitation [12,13]. They explained that the small polarons formed after CT excitation destabilize the generalized Peierls phase. It is reported that the visible absorption band in the K-TCNQ crystal is due to the π-π^* transition [21,22], therefore in the present experiment, π-π^* state is excited. The present experiment shows that it also leads to the melting of generalized Peierls phase in the same way as the CT excitation. Then, correspondence between both relaxation times of the results indicate the relaxation from the π-π^* state in TCNQ to the CT state in the K-TCNQ crystal.

Figure 3 shows the vibrational spectra obtained by the FFT analysis. The high frequency modes were observed with the 9.4 fs NOPA pulse laser in the visible region. The vibrational structures of the TCNQ studied in previous papers show that TCNQ has 10 totally symmetric vibrations modes, including a 148 and 337 cm^{-1} mode [23–25]. The low frequency oscillations of about 100, 200, and 350 cm^{-1} are two intramolecular vibrations and an intermolecular oscillation, or crystal vibrations, and the all high frequency vibrations about 1200, 1400, and 1600 cm^{-1} are intramolecular vibrations. The results of these analyses are consistent with the results obtained by previous Raman scattering experiments and calculations. The vibration about 1200 cm^{-1} was assigned to the C-H in-plane bending mode (the in-plane bending mode of C-H), and those about 1400 and 1600 cm^{-1} were assigned to the stretching mode in the benzene ring and periphery double bonds, respectively [23,24]. In addition, the 1400 cm^{-1} vibration is an antisynchronous mode between benzene ring and periphery double bonds; on the other hand, the 1600 cm^{-1} vibration is a synchronous mode between these two.

The spectrogram analysis reveals that the instantaneous vibrational frequencies change with the delay time as in Fig. 6 [26]. The change has the following three features. First, the intermolecular vibration energies instantly change to lower energies as large as about 10 cm^{-1} after laser irradiation. The vibration frequency near 1600 cm^{-1} changes to 1592 cm^{-1} from the crystal Raman frequency 1603 cm^{-1}. Second, the frequencies in the intramolecular vibrations initially increased up as large as about 50 cm^{-1} to 500 fs after the laser excitation, and then decreased. For example, the frequency about 1600 cm^{-1} increased from ~1580 cm^{-1} at 100 fs to ~1630 cm^{-1} at 580 fs around the 2.22–2.18 eV energy region in Fig. 6. After that, the frequency decreased to ~1605 cm^{-1} at 1600 fs. Third, the vibrations with the frequencies of 1400 and 1600 cm^{-1} are frequency modulated at a period of nearly 510 fs. FFT spectrum of the $\Delta R/R$ spectrum in 2.22–2.18 eV in Fig. 7(a) shows the intermolecular oscillation frequency ~65 cm^{-1}. The frequency coincides with the frequencies in the FFT analysis of the two vibrational frequencies in the spectrogram ~1600 and ~1400 cm^{-1} in Figs. 7(b) and 7(c).

These features, an instant frequency change of 10 cm^{-1}, increase up to 500 fs by 50 cm^{-1} and frequency modulation

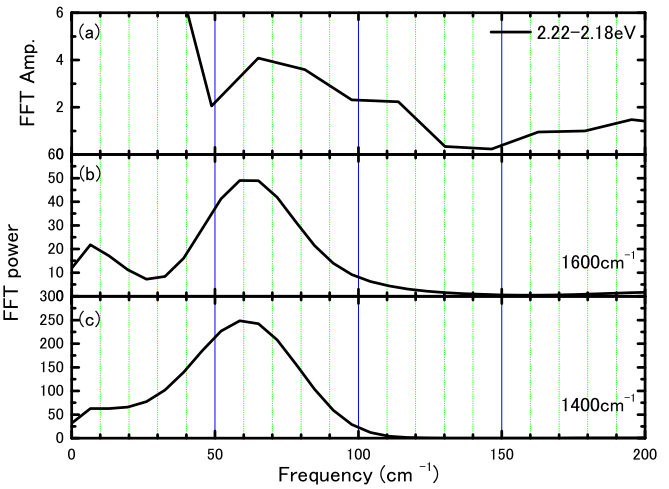

FIG. 7. (Color online) (a) The FFT analysis of the $\Delta R/R$ spectrum and (b) and (c) the modulated frequency in the spectrogram analysis in time delay in 500–1800 fs.

can be discussed as follows. Environmental factors including temperature change might cause the vibrational frequency change as a result of the structural change in the crystal which modifies the molecular state, shape, and interaction in TCNQ molecules. The instantaneous frequency change of 10 cm^{-1} just after photoexcitation is, however, too large to be induced by the change in the environments because the crystal structure and phase cannot be changed within 10 fs. Instead, the instantaneous frequency change is probably due to the contribution of the excited state. The molecular vibration modes of 1600 and 1400 cm^{-1} are assigned to in-phase and out-of-phase stretching modes of the double bonds in the TCNQ molecules [23,24]. The π-π^* excitation to the antibonding state from the bonding state of the TCNQ molecules reduces the bond order of the double bonds and leads to the decrease in the frequencies of those intramolecular vibrations.

It is unlikely that the vibrational frequency change as large as about 50 cm^{-1} is induced by the local temperature increase because 500 fs is too short for the lattice to be thermalized. Rather, it is considered to be caused by partial melting of the generalized Peierls phase with laser irradiation. This means that the modulation of the intramolecular vibration frequencies is induced by the change in the intermolecular distances between the molecules in the K-TCNQ crystal by the crystal oscillation, as described in detail as follows.

The frequencies of the modes of about 1600 and 1400 cm^{-1} increase between 0 and ~500 fs within τ_2 in Fig. 6. This is caused by the melting in the generalized Peierls phase by the following mechanism: The π electrons in the double bond of the molecules in the Peierls phase of the crystal are delocalized by dimerization, resulting in the redshift of intramolcular vibration frequencies. The K-TCNQ crystal has face-to-face stacking of the TCNQ molecules with a little tilt and the π electrons easily transfer to the neighboring TCNQ single bond from the double bond in the Peierls dimer. The tilted structure is one of the reasons that the order of the double bond is reduced in the crystal. After the melting of dimerization, the coupling between Peierls dimer molecules is reduced. Then, the bond order of the double bond in the TCNQ molecules is enhanced with the result that the frequencies of both vibrations are increased to those for the isolated molecules. In other words, the frequency increases are due to relaxation from the π-π^* excited state to the CT state, as shown in Fig. 1, of the TCNQ in 500 fs for the Peierls dimer to be melted.

Both frequencies of the modes about 1600 and 1400 cm^{-1} reach the maxima around 500 fs and then decrease toward the crystal Raman frequencies. This indicates recovering from the melted generalized Peierls phase to the dimerized phase, reducing the bond order of the double bonds induced by an increase of the contribution of charge resonance. The reduction of the bond order leads to the decrease in the intramolecular vibration frequencies. Vibrational frequencies in the TCNQ molecules of the generalized Peierls dimer are changed by those in the isolated molecules by recovering from the melting of the Peierls phase with laser irradiation.

The difference in the Raman frequencies between the K-TCNQ crystalline sample and TCNQ dissolved in acetonitrile are described in Ref. [24]. The frequency changes of the modes of 1400 and 1600 cm^{-1} are shown in Fig. 6. The frequencies of the 1600 and 1400 cm^{-1} in the crystal are lower than the corresponding peaks observed in the acetonitrile solution. Raman spectrum has peaks at 1615 (strong), 1604 (weak), and 1391 cm^{-1} in solution and 1625 (weak), 1603 (strong), and 1388 cm^{-1} in crystal in Ref. [27]. Judging from this result, the dominant vibration frequency near 1600 cm^{-1} is presumably different between the generalized Peierls dimer and single anions.

The molecular vibration in the K-TCNQ crystal is considered to be sensitive to the distance from the molecules in the neighboring columns because of charge-transfer interaction and van der Waals interaction. Therefore, the vibration frequencies are considered to recover to the stable frequencies in the Peierls phase in the longer delay time than the decay of generalized Peierls. In this recovering period there is 510 fs (=65 cm^{-1}) modulation in the instantaneous frequencies. This is probably due to the TO phonon mode as follows: Ikegami *et al.* reported the intermolecular oscillation with the frequency of 20 cm^{-1} (=1.7 ps) due to the LO phonon mode, and the oscillation is induced by melting of the Peierls phase [12,13]. In our experiment, in contrast, the modulation frequency in the spectrogram in Fig. 6 is not 20 cm^{-1} but 65 cm^{-1}. The origin of the difference is probably difference in the phonon mode of the intermolecular oscillation. They reported the polarized Raman scattering spectra of K-TCNQ in Fig. 11 of Ref. [13]. The 20 cm^{-1} oscillation is observed in the setup with the polarization of the excitation laser and scattered light both parallel to the crystal axis. This result indicates that the oscillation direction parallel to the molecular stacking axis, or the crystal oscillation corresponds to the LO phonon mode. On the other hand, the same figure shows that the 65 cm^{-1} oscillation with the polarization of the scattered light perpendicular to that of the excitation laser and the crystal axis. It is important to note that in our experiment the electric field of the NOPA pulse is perpendicular to the crystals stacking axis as shown in Fig. 1. Thus, the 65 cm^{-1} oscillation can be safely assigned to the TO phonon mode in intermolecular oscillation. In other words, TCNQ molecules vibrate to the vertical direction of the crystal axis with the frequency of 65 cm^{-1}.

Our result indicates that intramolecular vibration with frequency of the 1400 and 1600 cm^{-1} are modulated with the crystal phonon mode of 65 cm^{-1}, whose oscillation direction is perpendicular to the stacking axis, induced by the melting of the Peierls phase by the laser excitation.

V. CONCLUSION

The pump-probe reflectance in the K-TCNQ crystals was studied with the 9.4 fs visible pulse laser. The molecular vibrations have mainly three frequency components around 1200, 1400 and 1600 cm^{-1}. These frequencies are consistent with the previous Raman spectra and calculations. Thus, these vibrational modes are identified to the intramolecular vibrations. First, the frequencies decrease instantly upon laser irradiation with π-π^* excitation of the TCNQ molecules. Following this, the vibrational frequencies increase with generating polaron at the time constant $\tau_2 \sim 500$ fs and then decrease with recovering generalized Peierls phase. The frequencies change can be explained in terms of the change of the population interaction and the bond order of the double

bonds. These vibrational frequencies are modulated by the TO phonon mode at 65 cm^{-1} with short pulse laser excitation because of the contribution of the intermolecular oscillations with the vertical direction of the stacking axis in the crystal. The crystal modulation is caused by the change in the interaction of the coupled TCNQ molecules due to the distance change between molecules with the melting of the Peierls phase.

[1] S. Koshihara and S. Adachi, J. Phys. Soc. Jpn. **75**, 011005 (2006).

[2] S. Ohkoshi, H. Tokoro, and K. Hashimoto, Coordination Chem. Rev. **249** 1830 (2005).

[3] F. Schmitt, P. S. Kirchmann, U. Bovensiepen, R. G. Moore, L. Rettig, M. Krenz, J.-H. Chu, N. Ru, L. Perfetti, D. H. Lu, M. Wolf, I. R. Fisher, and Z.-X. Shen, Science **321**, 1649 (2008).

[4] J. W. Bray, L. V. Interrante, I. S. Jacobs, and J. C. Bonner, in *Extended Linear Chain Compounds*, edited by J. S. Miller, Vol. 3 (Plenum, New York, 1983), p. 353.

[5] M. Konno, T. Ishii, and Y. Saito, Acta Crystallogr. Sect. B **33**, 763 (1977).

[6] J. P. Lowe, J. Am. Chem. Soc. **102**, 1262 (1980).

[7] J. Richard, M. Vandevyver, P. Lesieur, A. R. Teixier, A. Barraud, R. Bozio, and C. Pecile, J. Chem. Phys. **86**, 2428 (1987).

[8] B. D. Silverman, J. Chem. Phys. **70**, 1614 (1979).

[9] J. G. Vegter, T. Hibma, and J. Kommandeur, Chem. Phys. Lett. **3**, 427 (1969).

[10] Y. Toda, K. Tateishi, and S. Tanda, Phys. Rev. B **70**, 033106 (2004).

[11] H. Okamoto, Y. Ishige, S. Tanaka, H. Kishida, S. Iwai, and Y. Tokura, Phys. Rev. B **70**, 165202 (2004).

[12] H. Okamoto, K. Ikegami, T. Wakabayashi, Y. Ishige, J. Togo, H. Kishida, and H. Matsuzaki, Phys. Rev. Lett. **96**, 037405 (2006).

[13] K. Ikegami, K. Ono, J. Togo, T. Wakabayashi, Y. Ishige, H. Matsuzaki, H. Kishida, and H. Okamoto, Phys. Rev. B **76**, 085106 (2007).

[14] S. Iwai and H. Okamoto, J. Phys. Soc. Jpn. **75**, 011007 (2006).

[15] L. Luer, C. Manzoni, G. Cerullo, G. Lanzani, and M. Meneghetti, Phys. Rev. Lett. **99**, 027401 (2007).

[16] H. Uemura, H. Matsuzaki, Y. Takahashi, T. Hasegawa, and H. Okamoto, J. Phys. Soc. Jpn. **77**, 113714 (2008).

[17] H. Uemura, H. Matsuzaki, Y. Takahashi, T. Hasegawa, and H. Okamoto, Physica B **405**, S357 (2010).

[18] A. Shirakawa and T. Kobayashi, Appl. Phys. Lett. **72**, 147 (1998).

[19] A. Shirakawa, I. Sakane, and T. Kobayashi, Opt. Lett. **23**, 1292 (1998).

[20] A. Baltuska, T. Fuji, and T. Kobayashi, Opt. Lett. **27**, 306 (2002).

[21] H. T. Jonkman and J. Kommandeur, Chem. Phys. Lett. **15**, 496 (1972).

[22] K. Yakushi, T. Kusaka, and H. Kuroda, Chem. Phys. Lett. **68**, 139 (1979).

[23] D. L. Jeanmaire and R. P. Van Duyne, J. Am. Chem. Soc. **98**, 4029 (1976).

[24] I. Zanon and C. Peclle, J. Phys. Chem. **87**, 3657 (1983).

[25] R. Bozio and C. Pecile, in *Advance Spectroscopy*, edited by R. J. H. Clark and R. E. Hester, Vol. 19 (Wiley, New York, 1991), p. 1.

[26] See Supplemental Material at http://link.aps.org/supplemental/10.1103/PhysRevB.90.085119 for the spectrogram analysis including in investigation of the significant artifacts.

[27] K. D. Truong and C. Carlone, Phys. Rev. B **20**, 2238 (1979).